



Changes in Retinal Time Scale Under Background Light: Observations on Rods and Ganglion Cells in the Frog Retina

KRISTIAN DONNER,* ARI KOSKELAINEN,† KAJ DJUPSUND,* SIMO HEMILÄ†

Received 17 March 1994; in revised form 3 November 1994

The kinetics of rod responses to flashes and steps of light was studied as a function of background intensity (I_B) at the photoreceptor and ganglion cell levels in the frog retina. Responses of the rod photoreceptors were recorded intracellularly in the eyecup and as ERG mass potentials across the isolated, aspartate-superfused retina. The kinetics of the retinally transmitted signal was derived from the latencies of ganglion cell spike discharges recorded extracellularly in the eyecup. In all states of adaptation the linear-range rod response to dim flashes could be modelled as the impulse response of a chain of low-pass filters with the same number of stages: 4 (ERG) or 4–6 (intracellular). Dark-adapted time-to-peak (t_p , mean \pm SD) at 12°C was 2.4 ± 0.6 sec (ERG) or 1.7 ± 0.4 sec (intracellular). Under background light, the time scale shortened as a power function of background intensity, I_B^{-b} with $b = 0.19 \pm 0.03$ (ERG) or 0.14 ± 0.04 (intracellular). The latency-derived time scale of the rod-driven signal at the ganglion cell agreed well with that of the photoreceptor responses. The apparent underlying impulse response had $t_p = 2.0 \pm 0.7$ sec in darkness and accelerated as I_B^{-b} with $b = 0.17 \pm 0.03$. The photoreceptor-to-ganglion-cell transmission delay shortened by 30% between darkness and a background delivering *ca* 10^4 photoisomerizations per rod per second. Data from the literature suggest that all vertebrate photoreceptors may accelerate according to similar power functions of adapting intensity, with exponents in the range 0.1–0.2. It is noteworthy that the time scale of human (foveal) vision in experiments on flicker sensitivity and temporal summation shortens as a power function of mean luminance with $b \approx 0.15$.

Rod photoreceptor Ganglion cell Retina Visual adaptation Temporal resolution Temporal summation Sensory latency

INTRODUCTION

The responses of photoreceptor cells to light increments and decrements become faster as the general illumination increases (Fuortes & Hodgkin, 1964; Baylor & Hodgkin, 1974; Baylor, Lamb & Yau, 1979; Forti, Menini, Rispoli & Torre, 1989; Kraft, Schneeweis & Schnapf, 1993). The improved high-frequency response of this most distal low-pass filter permits higher temporal resolution of the whole visual system, one of the ways in which the richer information potentially carried by larger numbers of photons is utilized. Here we measure changes in the kinetics of linear-range rod responses over a wide range of background illumination. Our main purpose, beside precise description, is to clarify how far changes of time scale at the photoreceptor level can explain those at the retinal output (derived from ganglion cell response latencies). The general goal is to

understand the mechanisms underlying the acceleration of vision with increasing mean illumination.

We find that the shortening of time scale at both the photoreceptor and the ganglion cell level is well described by similar power functions of background intensity. A power-function relation between rod photoreponse time scale and *sensitivity* (Fuortes & Hodgkin, 1964; Baylor & Hodgkin, 1974; Baylor, Matthews & Yau, 1980) holds somewhat less well. Response acceleration, but not sensitivity adaptation, levels off at backgrounds delivering more than 1000 photoisomerizations per rod per second [$Rh^* \text{ sec}^{-1}$]. In adaptation to stronger backgrounds, mechanisms that act by speeding up response recovery, thus affecting both sensitivity and time scale (see e.g. Fain & Cornwall, 1993), are evidently superseded by gain controls not coupled to time scale.

Published data on other vertebrate photoreceptors suggest that acceleration according to power functions of mean illumination with exponents between 0.1 and 0.2 may be a universal rule. Moreover, the time scale of human foveal vision as measured in experiments on

*Department of Biosciences and Department of Ecology and Systematics, University of Helsinki, FIN-00014 Helsinki, Finland.

†Laboratory of Physics, Helsinki University of Technology, FIN-02150 Espoo, Finland.

temporal summation and flicker sensitivity depends on mean luminance in similar manner (Roufs, 1972). The present result, that time scale changes at the retinal output reproduce those in photoreceptors with the addition only of a minor shortening of the retinal transmission time, supports the idea that psychophysical time scale changes predominantly reflect photoreceptor kinetics.

METHODS

Animals and preparation

Common frogs, *Rana temporaria*, were caught in the autumn either in SW Finland or in Leningrad Region (Russia). They were kept in near-darkness in basins at *ca* 4°C without feeding (resembling natural hibernating conditions). On the evening before an experiment the frog was transferred to a water-cooled bucket in a dark room where it was allowed to warm overnight to about 15°C.

Preparation was carried out in dim red light. The frog was double-pithed, the eyes were enucleated and opened along the equator, and the anterior portion was removed. For ERG, the retina was isolated in cooled Ringer and placed in a holder where it was superfused on the receptor side (see Donner, Hemilä & Koskelainen, 1988). For intracellular rod recordings and extracellular ganglion cell recordings, the vitreous was drained to a depth of 0.1–0.3 mm and the intact eyecup was placed in a cooled recording chamber without perfusion (see Copenhagen, Donner & Reuter, 1987). Temperature was 11–12°C in all experiments except in four of the ERG experiments.

Intracellular recording

Recording. Rods were penetrated with glass capillaries (Brown-Flaming puller, Sutter Instruments) filled with 0.5 M K-acetate and 0.5 M K-methylsulphate (resistance 0.5–1 GΩ) and advanced through the retina with a micromanipulator (Narishige). Photoresponses were d.c.-recorded, amplified (Axoclamp 2A, Axon Instruments) and stored on tape (TEAC FM recorder) and in digital form on a computer hard disk. Rods were distinguished from cones, horizontal cells and hyperpolarizing bipolar cells on the basis of spectral sensitivity, changes in response waveform with changing stimulus wavelength, receptive field size, and presence or absence of a transient hyperpolarizing “nose” in responses to brighter flashes (see e.g. Brown & Pinto, 1974; Belgum & Copenhagen, 1988).

Optics. In the single-channel optical system, light from a 50 W halogen lamp (Osram) driven by a stabilized current source formed a homogeneous field on the retina after passing through heat-absorbing filters, interference filters (Schott DIL), neutral density filters (Balzers) and a circular 4-log-unit neutral-density wedge (Melles Griot). In darkness, stimuli were delivered by a computer-controlled shutter (Compur). In conditions with background light, the shutter was kept continuously

open and square-wave incremental pulses of desired contrast were delivered by swift deflections of the circular wedge driven by a strong computer-controlled motor (MAM 36/15, Mattke, Germany). The movement of the wedge took 4–8 msec for dim flashes and maximally 20 msec for stronger flashes; very strong flashes were produced by rotation in the opposite direction, which required no more than 5 msec. The characteristics and performance of the motor-wedge system and the computer control are described in detail elsewhere (Djup-sund, Kouvalainen, Järvilehto & Weckström, 1995). Stimulus duration was 100 msec. For linear-range responses of frog rods at the low temperature (11–12°C) of all the intracellular experiments this can be considered as a “brief flash” even under fairly strong backgrounds, where responses peaked at *ca* 500 msec (see Fig. 2). Although the finite duration of the pulse will in principle cause slight differences in the waveform of the earliest rise compared with responses to ideal “delta pulses”, this is of no great consequence, as fits to intracellular responses were based on the entire waveform. The circular test fields of 1 mm diameter (size controlled by a diaphragm inserted in the beam) represented full-field illumination to single rods.

The ERG mass rod potential

Recording. Our technique for recording ERG mass receptor responses across isolated retinas with synaptic transmission blocked by aspartate was as described by Donner *et al.* (1988). The isolated retina was superfused on the receptor side by a Ringer solution containing (mM): NaCl 95, KCl 3, CaCl₂ 0.9, MgCl₂ 0.5, glucose 10, Na-aspartate 2, and buffers sodium bicarbonate 6 plus sodium-HEPES 6. pH was adjusted (by adding NaOH or HCl) to 7.5. 5% Leibovitz culture medium L-15 (Sigma) was used in the Ringers to improve the viability of the retina. L-15 permitted successful recording at higher temperatures, where Donner *et al.* (1988) found that retinas deteriorated rather quickly.

Photoresponses were d.c.-recorded as a transretinal voltage with Ag/AgCl electrodes, digitized at 100 or 200 Hz and stored on a computer hard disk. The optical system had two channels. The spectral composition and intensity of the light were independently controlled with interference filters (Schott DIL) in the stimulus channel, the edge filter Schott RG 630 in the background channel, and neutral density filters (Schott) and wedges in both. Since the retina was mounted photoreceptors upwards, the light entered from the distal ends of rods. Stimuli were homogeneous full-field flashes (20 msec, i.e. “brief flashes”) delivered by a computer-controlled electromagnetic shutter (Compur).

ERG compared with intracellular recording. Most of the quantitative analysis of photoreceptor kinetics is based on ERG data. Intracellular voltage recording was used to supplement the ERG on points where the latter signal is problematic (see below) and to ascertain that the response most closely representing the signal transmitted to higher-order neurons would give essentially the same picture as the ERG. If this is the case, the ERG

technique has several advantages. Firstly, it is comparatively non-invasive, as the rods are neither penetrated (as in intracellular recording) nor teased apart from the retinal tissue (as in current recording from single cells). This is crucial when studying response kinetics, which is particularly vulnerable to disruptive treatments. Secondly, the signal is an ensemble average from tens of thousands of rods, hence has a high signal/noise ratio. This makes it possible to study responses to weak stimuli without extensive averaging. Thirdly, the ERG signal is the ohmic voltage associated with the *current* response of the rod and is unaffected by feedback mechanisms which (for our present purposes) “distort” membrane voltage responses (see Fig. 1).

On the other hand, although the rods in the isolated retina used for ERG were intact and embedded in tissue, they were of course detached from the pigment epithelium and exposed to artificial superfusate. Further, the transretinal ERG has its own weaknesses that must be clearly realized: (1) peculiar relations between tissue currents and the resulting voltage (Donner, Hemilä & Koskelainen, 1992), (2) contributions from other photoreceptors and (3) distortion of later parts of the responses by glial currents (for both the latter points, see Fig. 1).

Extracellular ganglion cell recording

Action potentials were extracellularly recorded with glass micropipettes filled with 3 mM NaCl (resistance *ca* 10 M Ω) from single ganglion cell somata or axons in the eyecup preparation. The eyecup was kept in a moist chamber at 11–12°C, whereby stable recording from the same cell for 10 hr or more could be achieved without oxygenation or perfusion. In a two-channel optical system, interference filters (Schott DIL) and neutral density filters (Balzers) and wedges could be independently inserted to provide background and stimulus lights of desired wavelengths and intensities. Circular test spots were produced by inserting masks into the beam. Square-wave light pulses of desired duration were delivered by a Compur electronic shutter. The interstimulus interval was 30 or 45 sec depending on the state of adaptation and the intensity of the stimulus. To isolate rod-driven responses over as wide intensity ranges as possible, backgrounds were yellow or red (i.e. cone-suppressing, 558 or 615 nm) while stimuli were blue-green (i.e. rod-favouring, 495 or 512 nm). All results refer to ON-responses (recorded from ganglion cells of classes 1–3), which correspond to the leading edge of the photoreceptor hyperpolarization (see Donner, 1989).

Light calibrations

Rates of isomerizations in red rods. All stimulus lights were calibrated in units of incident quanta per mm² sec⁻¹ with an Airam UVM-8 radiometer or a calibrated pin diode placed in the position of the retina (see Koskelainen, Hemilä & Donner, 1994). This was converted into *numbers of photoisomerizations per rod per second* (Rh* sec⁻¹) as follows. The mean density of rhodopsin rods in *R. temporaria* is 15,700 mm⁻² and the mean

length and diameter of the roughly cylindrical outer segments 43 and 6.4 μ m, respectively (Hemilä & Reuter, 1981). The mean optical density of 20 good isolated retinas measured as described by Gyllenberg, Reuter and Sippel (1974) was 0.344. Assuming a quantum efficiency for isomerization of 0.66 (Dartnall, 1972), 36% of 502-nm photons incident on the retina produce isomerizations in rhodopsin rods. Rates of isomerizations from other wavelengths are lower in proportion to the lower absorbance of rhodopsin₅₀₂.

Analysis

The dim-flash rod response. Dim-flash rod responses were fitted with the “independent activation” model of Baylor, Hodgkin and Lamb (1974a). Although the model must now be regarded as purely phenomenological, it provides a good description of response waveforms in a large number of species. The model of Lamb and Pugh (1992), which relates the early rise of responses to phototransduction *mechanisms* differs only marginally as regards the predicted shape of the rising response (see Hood and Birch, 1993a, b).

The response $R_F(I, t)$ to a flash of intensity I [Rh* sec⁻¹] and (very short) duration t_F is [cf. equation (41) in Baylor *et al.* (1974a)]:

$$R_F(I, t) = S_F I t_F [n^n / (n-1)^{n-1}] e^{-t/\tau} (1 - e^{-t/\tau})^{n-1} \quad (1)$$

where t is time after flash. The parameters are: (1) the absolute flash sensitivity S_F (peak response amplitude per Rh* in the linear response range), which scales response size; (2) the number of stages in the activation chain n , which determines the waveform of the response; (3) the time constant τ , which determines the overall time scale of the response. S_F was determined by fitting Michaelis functions (in darkness: modified Michaelis functions) to three-point intensity–response data as described by Donner, Hemilä and Koskelainen (1989).

Describing the time–course of a recorded response by equation (1) implies fixing values for n and τ . One result of the experiments to be described was that n could, to a first approximation, be considered as independent of background intensity (see Figs 2 and 3). Since n and τ are interdependent and our main purpose was to measure changes in τ , we therefore constrained n to have a constant value for one cell (in ERG, for one retina) under all backgrounds. The time scale is then completely captured by τ or any well-defined time criterion, such as the time when the response has risen or fallen back to a certain proportion of its maximum amplitude. A particularly convenient measure is the time-to-peak (t_p) of the flash response [obtained by differentiation of equation (1) and setting $dR_F(I, t_p)/dt = 0$]:

$$t_p = \tau \ln n. \quad (2)$$

Ganglion cell L-functions. The response latency of ganglion cells (L) was measured as the time from the onset of a step-of-light stimulus to the midpoint of the first spike. Step stimulation (5 sec square-wave pulses) was used in order to extend the available range of purely rod-driven responses (before cone intrusion at high

stimulus intensities). It is assumed that the ganglion cell always fires the first spike at a moment when the rod response summed over its whole receptive field has reached a fixed criterion (*threshold*) amplitude R_T and been transmitted through the retina. The step response of the rods, $R_S(I, t)$, is essentially the time integral of the flash response in equation (1) [cf. equation (40) of Baylor *et al.* (1974a, b)]:

$$R_S(I, t) = SI(1 - e^{-t/\tau})^n \quad (3)$$

where S is step sensitivity (final response amplitude per $\text{Rh}^* \text{sec}^{-1}$ in the linear response range). Observe that:

$$S/S_F = t_i = \tau[n/(n-1)]^{n-1} \quad (4)$$

where t_i is the *integration* (or *summation*) time of the response.

We denote by $l = l(I)$ (*photoreceptor latency*) the time from stimulus onset in which the summed photoreceptor response rises to R_T , and by d the retinal transmission delay. Thus ganglion cell latency $L = l + d$. The step-stimulus intensity that elicits a rod response of *final* amplitude R_T (summed across the ganglion cell receptive field) is the *threshold intensity*, $I_T = R_T/S$, thus $R_T = SI_T$. Observing that $R_S = R_T$ when $t = l$ in equation (3) we obtain:

$$R_T = SI_T = SI(1 - e^{-l/\tau})^n. \quad (5)$$

Thus photoreceptor latency as function of stimulus intensity is:

$$l = -\tau \ln[1 - (I_T/I)^{1/n}]; \quad (6)$$

and ganglion cell latency as function of stimulus intensity:

$$L = l + d = d - \tau \ln[1 - (I_T/I)^{1/n}]. \quad (7)$$

We term this the *L-function*, $L = L(I)$. Fitting *L*-functions to recorded latencies allows estimation of the rod parameters n and τ as well as the retinal transmission delay d . For each cell in each state of adaptation, the data to be fitted consisted of a set of latencies to between 5 and 15 different stimulus intensities, usually spaced 0.5 log units apart (thus covering 2–7 log intensity units). Each latency was the mean obtained from at least 3 presentations of the same stimulus.

Threshold intensity I_T was first determined as the intensity to which the ganglion cell responded on 50% of the stimulus presentations (e.g. Donner, 1987a). After that, n was determined by fitting power functions to the latency data. This procedure, described in detail by Donner (1989), serves as an “objective” way of determining n . For ganglion cells as for rods, n was constrained to be constant in different states of adaptation, so for each cell the integer n that would on average provide the best description of all data sets was chosen. The transmission delay d was then determined by an iterative procedure where a tentative d value was first subtracted from each latency, transforming the data into a set of $L - d$ values. Rearranging equation (7) gives:

$$\tau = -(L - d)/\ln[1 - (I_T/I)^{1/n}]. \quad (8)$$

Thus each of the $L - d$ values provides an independent estimate for τ . Ideally, all estimates from one cell under one background should coincide. A natural criterion for choosing d was therefore to take the value that would *minimize the variance* of τ -estimates within a data set. This d -value was found by trying different values (with a resolution of 5 msec). The final τ -estimate for one cell in one state of adaptation was the mean of these least-variance estimates from the relevant data set.

For more detailed justification of the procedures the reader is referred to Donner (1989).

RESULTS

Rod acceleration under background: general properties of intracellular and ERG responses

A qualitative idea of how flash responses of rods accelerate under background light is given by Fig. 1, where the upper panels show the “dark” situation and the lower panels the “background” (100 or 150 $\text{Rh}^* \text{sec}^{-1}$) situation. The figure also illustrates the differences between responses recorded by the two techniques we used: the left-hand panels show intracellular voltage records from one rod, the right-hand panels ERG mass potentials from one retina. With both techniques it is clear that the rising phase of all responses, as well as the return to baseline of *small* responses, are accelerated by backgrounds.

For large responses the picture is more complicated, revealing significant differences between intracellular and ERG responses. The former show a fast initial relaxation from peak, particularly under background light [Fig. 1(C)]. This is due to feedback mechanisms that do not affect the *photocurrent* and thus not the ERG (Baylor *et al.*, 1974a, b; 1979; Schwartz, 1976; Cervetto, Pasino & Torre, 1977; Detwiler, Hodgkin & McNaughton, 1980). ERG responses are instead distorted by two components of non-rod origin. First, the late parts especially of larger responses are contaminated by glial currents obscuring the actual time-course of the photoreceptor component (e.g. Tomita & Yanagida, 1981). Second, under stronger adapting backgrounds a distinct cone response [sharp peak in Fig. 1(D)] rides on top of the rod response to brighter flashes.

In this paper we restrict our attention to the kinetics of small, *linear-range* responses. Linearity of phototransduction in a low-intensity (or low-contrast) stimulus range implies that response amplitude grows in direct proportion to the numbers of photoisomerizations received, while the waveform and kinetics stay constant (see e.g. Pugh & Lamb, 1990). Responses to dim, brief flashes of light thus (ideally) reproduce the waveform of the elementary response to a single photoisomerization.

Changes in the time scale of dim-flash voltage responses

Figure 2 shows dim-flash responses from one rod recorded in darkness (A) and against 3 backgrounds delivering 1, 10 and 100 $\text{Rh}^* \text{sec}^{-1}$, respectively (B–D). The smooth curves trace equation (1) with the number

of stages constrained to be the same ($n = 4$) under all backgrounds. They are seen to provide reasonable fits to all responses, implying that response shape stays roughly constant. The difference when going from (A) to (D) is that the time scale shortens (and sensitivity decreases). These central observations were confirmed in 7 rods studied under at least 3 background intensities. The best-fitting n -value varied between 4 and 6.

Although the responses in Fig. 2 are averages of many single records, they are still rather noisy. The basic

reason is that we have to consider responses of very small amplitude, as only these can be trusted to be broadly unaffected by voltage feedback mechanisms (see above). Accurate model-fitting to such small responses, however, would really require much more extensive (time-consuming) averaging. For determination of parameters under a large number of background intensities, we therefore mainly relied on the leading edge of ERG responses, which may be preferable in other respects as well (see Methods).

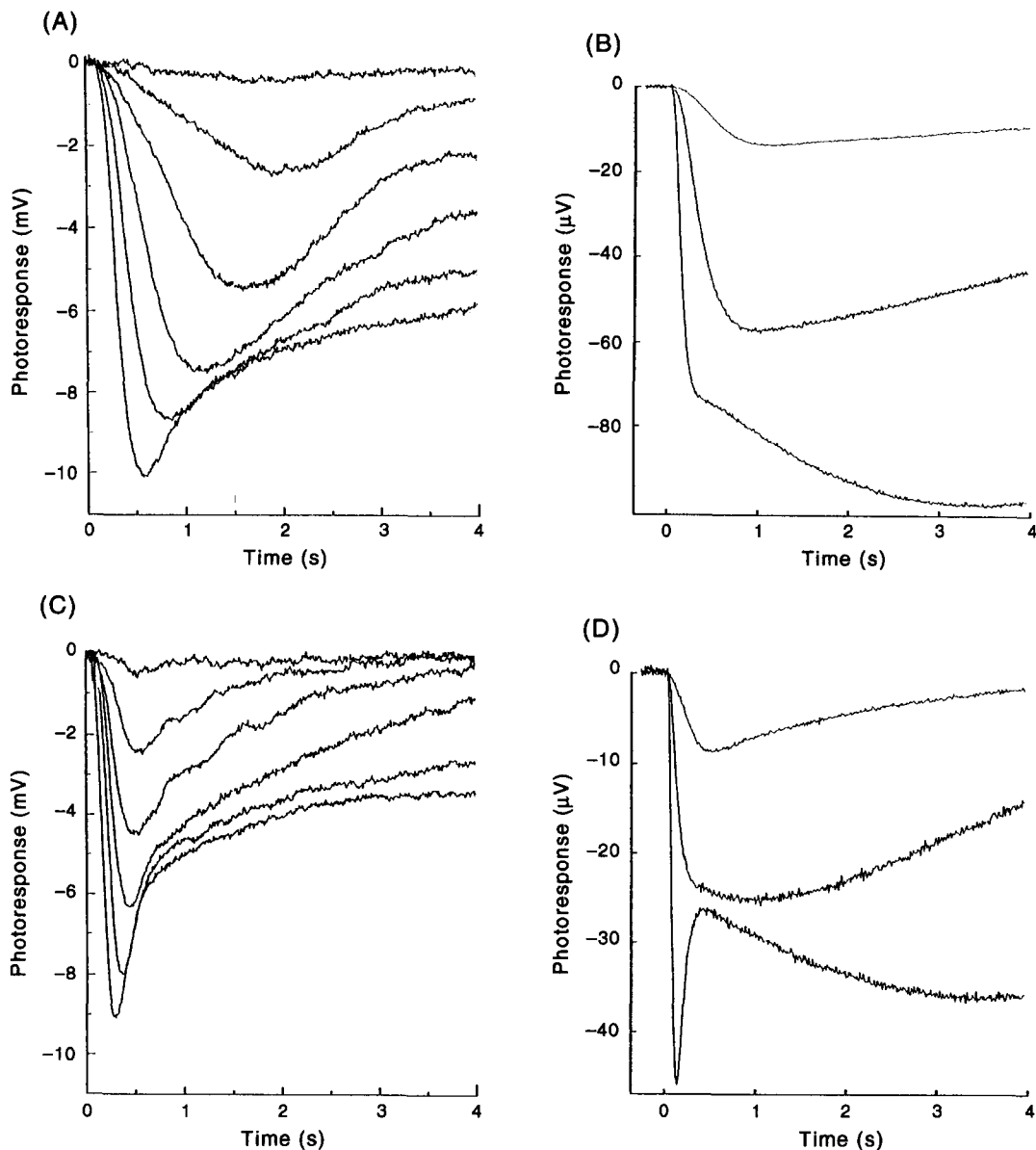


FIGURE 1. Families of intracellular (A, C) and ERG (B, D) rod responses to brief flashes of light in darkness (A, B) and in the presence of background illumination (C, D): $I_B = 100 \text{ Rh}^* \text{ sec}^{-1}$ in (C) and $150 \text{ Rh}^* \text{ sec}^{-1}$ in (D). (A, C) Intracellular rod photovoltages recorded in the eyecup. Background and flashes both 512 nm, flashes at 0.5 log unit intensity intervals starting from 1 Rh^* in (A) and 50 Rh^* in (C). All traces are averages of four single responses. Temperature 12°C. (B, D) ERG mass receptor potentials recorded across the isolated retina. Flashes at 1 log unit intervals starting from 22 Rh^* in (B) and 280 Rh^* in (D). The smallest responses are averages of eight, the other traces show single responses. Flashes 494 nm, background "red" edge filter transmitting above 630 nm (to suppress cones relatively more than rods). In all responses a protracted glial tail is evident (see particularly the slow dome-like potential peaking about 4 sec in the largest responses). At the highest stimulus intensity in (D), a large cone response (sharp peak) appears. Temperature 21°C.

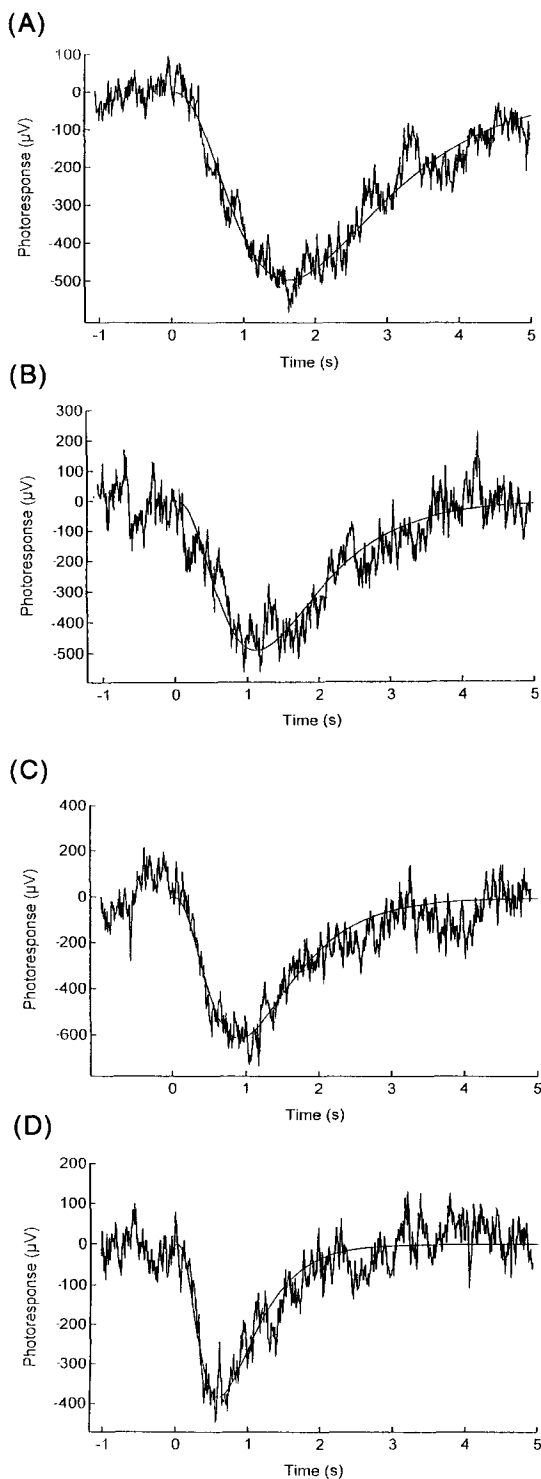


FIGURE 2. Linear-range responses recorded intracellularly in one rod in darkness (A) and against backgrounds delivering 1 (B), 10 (C) and 100 $\text{Rh}^* \text{sec}^{-1}$ (D). Nominal flash intensities [Rh^*]: 1.0 (A), 1.6 (B), 7.9 (C) and 50 (D). All traces are averages of 16 single responses. Smooth curves trace equation (1) with $n = 4$.

Changes in time scale and sensitivity of dim-flash ERG responses

Time scale vs background intensity. Figure 3 shows the early parts of ERG responses to linear-range flashes recorded from one retina [same as in Fig. 1(B) and (D)] in darkness and against two backgrounds [$1.5 \text{ Rh}^* \text{sec}^{-1}$

in (B) and $150 \text{ Rh}^* \text{sec}^{-1}$ in (C)]. As already pointed out, later parts of ERG responses, from peak or even earlier, are distorted by glial currents and therefore are neglected here. The smooth curves fitted to the leading edges trace equation (1) with the same number of stages ($n = 4$) in all cases. The consistently good fits support the idea that the shape remains invariant while the time scale and sensitivity change. Changes in kinetics can then be described by a single time parameter. In the following we use the time to peak (t_p) of the *model response* fitted to the leading edge of the recorded response.

Figure 4(A) shows (on log-log coordinates) how t_p changed with the state of adaptation in one retina. First consider the solid squares, which plot $\log t_p$ against $\log I_B$ (lower abscissa). Over a wide range of background

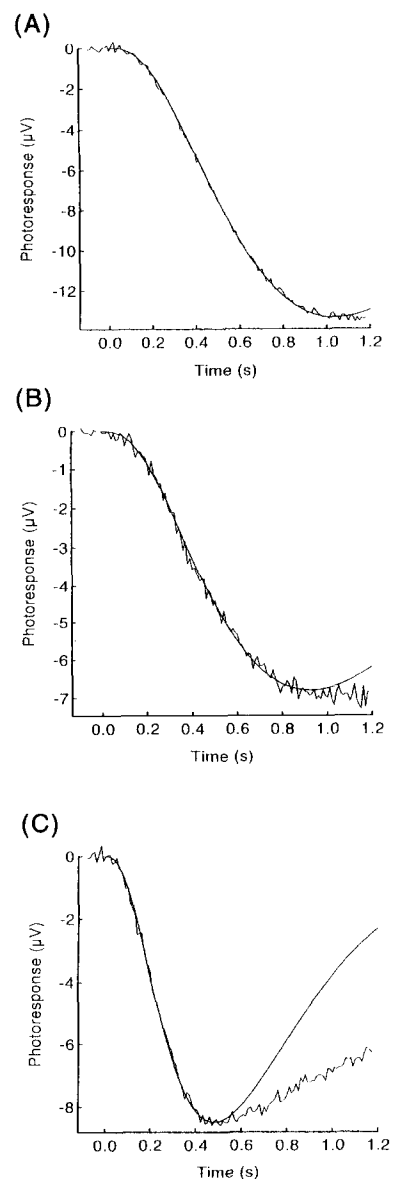


FIGURE 3. Linear-range ERG responses from one retina in darkness (A) and against backgrounds of intensities 1.5 (B) and 150 (C) $\text{Rh}^* \text{sec}^{-1}$. Flash intensities [Rh^*]: 22 in (A) and (B), 280 in (C). All traces are averages of eight single responses; (A) and (C) are the smallest responses in Fig. 1 (B) and (D) on expanded scales. Smooth curves trace equation (1) with $n = 4$. Temperature 21°C .

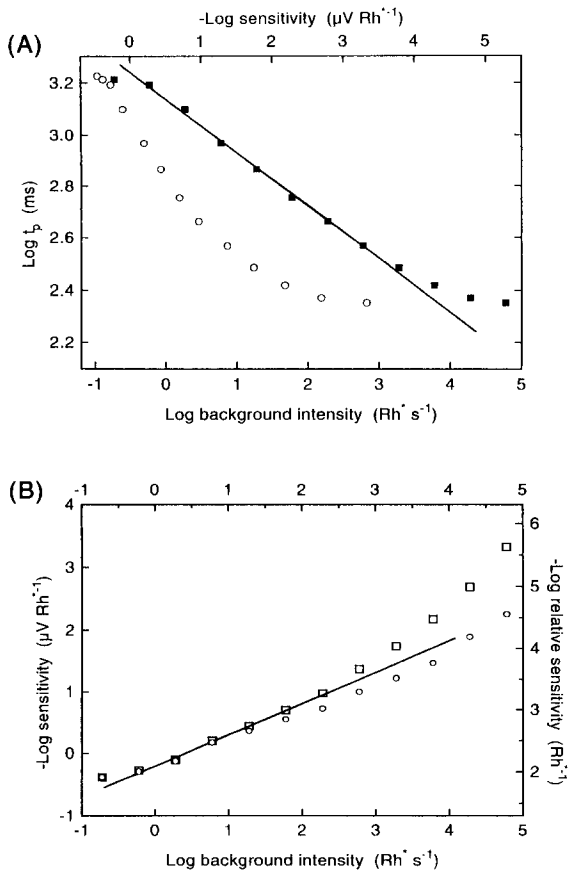


FIGURE 4. (A) Time scale of ERG responses under adapting backgrounds: $\log t_p$ plotted as function of $\log I_B$ (■, lower abscissa) and of $\log S_F$ (○, upper abscissa). The regression line has a slope of -0.206 . (The data point for the weakest background and those for the 3 highest backgrounds were not included in the fit.) (B) Sensitivity of ERG responses under adapting backgrounds: $\log S_F$ and $\log S_{F,\text{rel}}$ as functions of $\log I_B$ from the same experiment. The regression line fitted to the $\log S_F$ data below $\log I_B = 2.5$ has a slope of 0.51 . (Observe that changes of $\log R_{\text{max}}$ can be directly read from the figure as the difference between $\log S_{F,\text{rel}}$ and $\log S_F$.) Temperature 16.5°C .

intensities extending to at least $1000 \text{ Rh}^* \text{ sec}^{-1}$ they fall approximately on a straight line:

$$\log t_p = \log a - b \log I_B. \quad (9)$$

The regression coefficient is -0.206 ($r^2 > 0.99$) for the points included in the fit (see figure legend). In all 7 retinas studied, straight lines provided good fits to the log-log data ($r^2 > 0.97$ for all), with mean $b = 0.19 \pm 0.03$ (SD). Equation (9) is equivalent to:

$$t_p = a I_B^{-b}. \quad (10)$$

The change of rod response time scale in our ERG experiments can thus be described by a power function of background intensity with exponent -0.19 . Having established this, we fitted power functions also to time scale changes estimated from intracellular data. In 7 cells studied under the 1, 10 and $100 \text{ Rh}^* \text{ sec}^{-1}$ backgrounds (as in Fig. 2), the mean exponent for best fits was -0.14 ± 0.04 (SD), indicating a somewhat shallower background-dependence than for ERG responses. Factors likely to cause such a difference are considered in the Discussion.

It should be added that the ERG experiments were done under three different temperatures (three at 12°C , three at $16\text{--}17^\circ\text{C}$, and one at 21°C) to roughly explore whether the steepness of the $\log t_p - \log I_B$ relation might vary with temperature. No consistent temperature effect on b was detected, although dark-adapted response kinetics was about twice as fast at 21°C compared with 12°C .

Sensitivity vs background. Figure 4(B) shows how sensitivity changed with background in the same retina. First consider the dependence of (absolute) flash sensitivity, $\log S_F$, on $\log I_B$ (open squares, left-hand ordinate). This “threshold-vs-background-intensity” (TVI) function for flash responses closely follows “square-root” adaptation over a considerable range: the regression line shown for points below $\log I_B = 2.5$ ($I_B < 300 \text{ Rh}^* \text{ sec}^{-1}$) has slope 0.51 ($r^2 > 0.99$). The mean slope over this range in all 7 retinas was 0.54 ± 0.13 (SD) and the mean background intensity that depressed S_F by 50% from its dark-adapted value was $0.8 \pm 0.2 \text{ Rh}^* \text{ sec}^{-1}$. Under backgrounds stronger than $300 \text{ Rh}^* \text{ sec}^{-1}$ the adaptation curve steepened (see further below).

Time scale vs sensitivity. Next consider the relation between $\log t_p$ and $\log S_F$ (panel A, open circles, upper abscissa). This format has been used in several previous studies of time scale changes in photoreceptors (Fuortes & Hodgkin, 1964; Baylor & Hodgkin, 1974; Baylor *et al.*, 1980). Self-evidently, if $\log t_p$ and $\log S_F$ were both perfectly linear to $\log I_B$, their mutual relation would also be linear. In the particular case of TVI slope 0.5, the $\log t_p - \log S_F$ relation would be twice as steep as the $\log t_p - \log I_B$ relation. This is approximately true over the first 1.5 log units of sensitivity in Fig. 4(A). For all the 7 retinas studied, the linear part of the average $\log t_p - \log S_F$ relation would obviously have a slope of $0.19/0.54 \approx 0.35 \approx 1/2.8$. Baylor *et al.* (1980), fitting a swarm of $\log t_p$ vs $\log S_F$ data from many single toad rods by linear regression over a similar range, obtained the slope $1/2.65$. Thus, over a certain range, the relation of time scale to flash sensitivity can also be approximated by a power function, close to the prediction of the Fuortes-Hodgkin (1964) model where sensitivity and time scale are assumed to be *mechanistically* coupled so as to produce the relation:

$$t_p \propto S_F^{1/(n-1)}. \quad (11)$$

For $n = 4$ the slope should be $1/3$, not far from the observed $1/2.8$. From Fig. 4(A) it is evident, however, that the linear relation between $\log t_p$ and $\log S_F$ is a good approximation only over a limited range. The slope rather appears to be monotonically decreasing, suggesting that S_F is reduced also by mechanism(s) that do not simultaneously shorten the time scale of responses. A trivial mechanism of this kind would be response compression as the maximal response amplitude (R_{max}) begins to decrease under stronger backgrounds. This alone cannot, however, account for the changes, as seen from the plot of *relative* sensitivity ($S_{F,\text{rel}} = S_F/R_{\text{max}}$) as function of background in Fig. 4(B)

(open circles, right-hand ordinate). Relative sensitivity is a measure where effects of response compression have been factored out; it expresses the fraction of the total light-sensitive conductance turned off by one photoisomerization. The strong change of $S_{F,rel}$ in the range where time-scale changes level off ($I_B > 1000 \text{ Rh}^* \text{ sec}^{-1}$) therefore indicates that "Fuortes–Hodgkin-like" adaptation is gradually supplanted by a gain control not coupled to time scale.

Time scale of the rod signal after retinal transmission: ganglion cell recordings

Figure 5 shows four sets of latency vs. stimulus-intensity data, recorded from one ganglion cell in darkness and against 3 backgrounds spaced 1 log unit apart. The data are plotted on reciprocal ordinates to resolve the small differences between the short latencies at high stimulus intensities. The continuous curves are L -functions (see Analysis section) with $n = 5$ but differing in I_T , τ and d . As noted previously, reciprocal latencies ($1/L$) plotted against log intensity resemble straight lines, and these lines become steeper with light-adaptation (Donner, 1987b). From equation (7) it can be seen that, with n fixed, changes in the L -functions depend on: (1) rises of threshold intensity I_T , predominantly causing rightward shifts on the $\log I$ abscissa; (2) shortening of time scale (τ or t_p), predominantly causing upward shifts on the $1/L$ ordinate; (3) shortening of the transmission delay d , making the functions steeper.

Figure 6 decomposes the changes into these three basic factors. Panel (A) plots the increment threshold function, $\log I_T$ vs $\log I_B$, which rises via a square-root range to a final slope of 1.2. Such adaptation, somewhat steeper than the Weber relation (1.0), is common for the step thresholds of ganglion cells stimulated with moderately large test spots (Donner, 1981). Panel (B) shows how $\log t_p$ of the apparent underlying photoreceptor

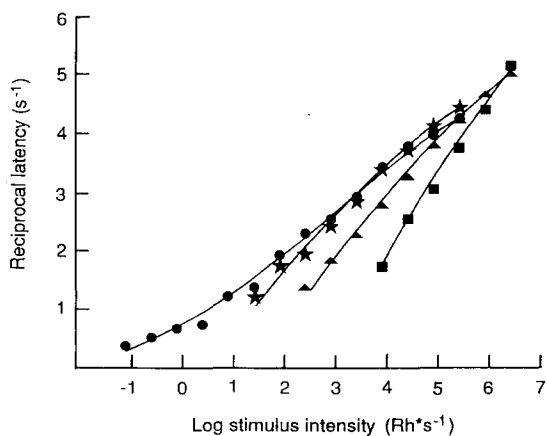


FIGURE 5. Reciprocal latency as function of stimulus intensity from one ganglion cell in darkness (●) and under different 558 nm backgrounds: 27 (★), 270 (▲) and 2700 (■) $\text{Rh}^* \text{ sec}^{-1}$. Abscissa: log intensity of increment step of light ($\text{Rh}^* \text{ sec}^{-1}$). Stimulus: 513 nm spot of diameter 0.30 mm, thus fully covering the 0.28 mm receptive field. The continuous lines are L -functions with $n = 5$ and parameters (τ , d) from left to right (1345, 170 msec), (405, 165 msec), (322, 150 msec) and (228, 125 msec).

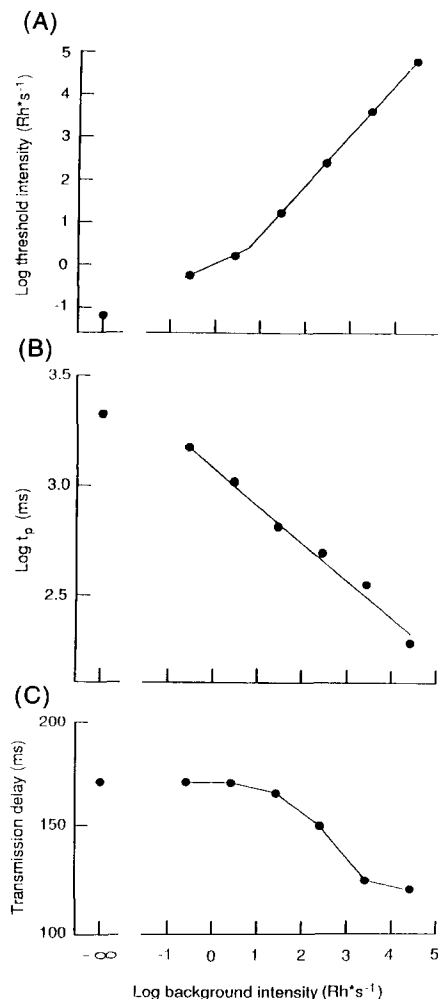


FIGURE 6. Changes in sensitivity and time parameters of the cell of Fig. 5. (A) Increment threshold function: log step threshold intensity ($\log I_T$) as a function of $\log I_B$. The two straight segments fitted by eye have slopes 0.5 and 1.2. (B) $\log t_p$ of the apparent underlying impulse response as a function of $\log I_B$. t_p was obtained from τ according to equation (2). The regression line has slope -0.17 . (C) Transmission delay d as a function of $\log I_B$. The lines have been drawn to connect the data points.

impulse response changed with background. On log–log coordinates, the data is fitted by a straight line with regression coefficient -0.170 ($r^2 = 0.98$). The mean slope from similar experiments on 7 cells was -0.17 ± 0.03 (SD) ($r^2 > 0.97$ for all fits). Obviously, this is in good agreement with the response acceleration observed in rods [equations (9) and (10) with $b = 0.17$].

Panel (C) shows how the transmission delay d shortened with increasing $\log I_B$. In 7 cells, the average decrease in d was by 30% over the full adaptation range, from 159 ± 23 msec in darkness to 114 ± 11 msec (different at $P < 0.01$, t -test for paired values). Under the strongest backgrounds cones are likely to intrude at high stimulus intensities, so the quantitative estimate might partly reflect a transition from slower rod transmission to faster cone transmission (Schnapf & Copenhagen, 1982). This cannot be the full explanation, however, because even under the strongest of our yellow backgrounds, rods determined responses to the blue-green

stimulus over a substantial range from threshold upwards [see Fig. 2 in Donner (1987a) where rod and cone thresholds are clearly distinguished]. At the moderate backgrounds where d already begins to change, there would be little if any cone involvement. The results thus suggest that the transmission of rod signals is indeed modified.

DISCUSSION

Response time scale in rods and ganglion cells

The time scale of the rod-driven excitation at the ganglion cell derived from latencies and that of the actual responses of the rod photoreceptors both contracted as power functions of background intensity, with no significant difference between exponents (-0.17 ± 0.03 in ganglion cells compared with -0.19 ± 0.03 for rod ERG responses and -0.14 ± 0.04 for intracellular rod responses). Response time scales at the two levels agreed in absolute terms as well. At 12°C , the time to peak of the apparent photoreceptor impulse response underlying dark-adapted ganglion cell responses was 2.0 ± 0.7 sec (\pm SD, 28 cells), compared with ERG rod $t_p = 2.4 \pm 0.6$ sec (7 retinas) and intracellular rod $t_p = 1.7 \pm 0.4$ sec (10 cells) [ERG data normalized to 12°C by applying $Q_{10} = 2.1$ (Donner *et al.*, 1988)].

Thus, ganglion-cell-derived values for both b and t_p were intermediate between rod values from intracellular and ERG recordings. On the other hand, the small although systematic differences between values obtained by the two latter techniques may be due to several known effects, some of which should (in the present context) properly be considered as experimental artifacts. In the intracellular dim-flash responses (Fig. 2), signal/noise did not permit accurate model-fitting to the leading edge alone. When the whole response is used, any remnant of the voltage-dependent feedback mechanisms considered in connection with Fig. 1 will shorten the apparent absolute time scale and probably weaken its background-dependence. [Note that the flash threshold of, for example, a dark-adapted ganglion cell may be 0.01 Rh* or less, thus a response to 1 Rh* in a dark-adapted rod as in Fig. 2(A) is not physiologically "small".] By contrast, ERG mass rod responses from the superfused retina are sensitive to several potentially decelerating factors, one being a relative overrepresentation of the slower response components from the distal ends of the rods (see Donner *et al.*, 1992). This "tip" component is known to be relatively most strongly depressed by background (Schnapf, 1983), which would enhance response acceleration.

Scotopic temporal summation in frogs, cats and humans

A functionally important temporal characteristic of ganglion cells is the time over which photon signals are integrated for a threshold response, the summation or integration time t_i . This can be measured independently, without relying on temporal properties of recorded re-

sponses, as the ratio of threshold intensities under flash and step stimulation, multiplied by flash duration (Baylor & Hodgkin, 1973). Under the independent activation model, t_i is related to τ by equation (4), implying (when n is constant) that t_i should show the same dependence on I_B as do τ and t_p . It is satisfying to note that the summation time of frog ganglion cells under background light has been found to decrease according to the power function $I_B^{-0.17}$ (Donner, 1987a), identical to that found here for the latency-derived time scale. This lends support to the linear model we have applied.

Interestingly, the summation time of cat ganglion cells appears to shorten in similar manner, roughly as $I_B^{-0.18}$, starting at a background intensity of about 3×10^5 quanta₅₀₇ deg⁻² sec⁻¹ (Fig. 7 in Barlow & Levick, 1969). This is roughly the I_B -range where individual cat rods *in situ* seem to start desensitizing (Steinberg, 1971; Sakmann & Fillion, 1972). Assuming that rod density is $400,000$ mm⁻², that 1 deg = 217 μm in the cat eye (Steinberg, Reid & Lacy, 1973) and that 25% of corneal 507-quanta produce isomerizations in rods (Barlow & Levick, 1969), 3×10^5 quanta₅₀₇ deg⁻² sec⁻¹ would correspond to 4 Rh* sec⁻¹, i.e. an intensity where each rod on average receives roughly one photoisomerization per integration time ($t_i \approx 300$ msec; see Tamura, Nakatani & Yau, 1989). Note that increment thresholds of cat ganglion cells start rising at 2–4 log units weaker backgrounds (Shapley & Enroth-Cugell, 1984). This suggests that scotopic time scale changes in mammals, too, originate in the rod photoreceptors.

In human rod vision, decrease of temporal summation (Sharpe, Stockman, Fach & Markstahler, 1993) and improvement of high-frequency flicker sensitivity (Sharpe, Stockman & MacLeod, 1989) require I_B -levels *ca* 3 log units higher than those where increment thresholds start rising. The minimum background intensity for affecting scotopic temporal summation seems to be around -0.5 – 0.0 log scot.td (Fig. 4 of Sharpe *et al.*, 1993), corresponding to 2–6 Rh* sec⁻¹. Again, this is consistent with a mechanism residing in the rods.

Sensitivity changes

Over a 2.5 log unit background range, rod ERG flash sensitivity adapted approximately as the square root of background intensity, the sensitivity-halving background being *ca* 0.8 Rh* sec⁻¹. Similar shallow adaptation has been found previously in mass receptor recordings from isolated frog retina [Figs 1–3 of Hood and Hock (1975) indicate average slope 0.5 over a corresponding range], but the conventional view from work on single rods is to regard it rather as a transition range towards a "proper", near-Weber dependence on I_B (Fain, 1976; Baylor *et al.*, 1980; Leibovic, Dowling & Kim, 1987). We wish to emphasize that the wide range of square-root adaptation observed here is not likely to be an artifact peculiar to the mass response of a heterogeneous population of superfused rods, because rod-driven flash thresholds of ganglion cells in the intact eyecup also follow a slope of approx. 0.5 up to about the same limit (*ca* 200 Rh* sec⁻¹: Reuter, Donner &

Copenhagen, 1986; Donner, 1987b). This is far beyond the background range where square-root adaptation can be interpreted as photon-limited flash detection by the ganglion cell itself, and is thus likely to reflect changes in rod sensitivity. [See Donner *et al.* (1990), who, however, monitored step thresholds.] Under dim and moderate backgrounds where protection from saturation is not yet a primary concern, square-root adaptation would in fact seem "ideal" for a rod, reducing response amplitudes by no more than is necessary to keep the output noise constant while photon fluctuations increase in proportion to $\sqrt{I_B}$.

Two types of background adaptation

The comparison of changes in sensitivity and time scale (Fig. 4) clearly reveals that two different types of background adaptation processes are present in rods, only one of which is associated with acceleration of photoresponses. Under low to moderate I_B , corresponding to the range of square-root adaptation, a relation between sensitivity and time scale approximating that foreseen by the Fuortes-Hodgkin model was observed (described by $t_p \propto S_F^{1/2.8}$). With increasing I_B , however, a progressively larger proportion of the sensitivity changes expressed a process that decreases the gain of phototransduction without affecting time scale. (The latter type of adaptation should not be confused with *response compression* due to decreasing R_{max} , which is a third factor that affects the size of responses and thus S_F).

Both types of adaptation might ultimately depend on the decreases in intracellular calcium ($[Ca^{2+}]_i$) known to accompany responses to light (see Pugh & Lamb, 1990; Fain & Cornwall, 1993). Lowered $[Ca^{2+}]_i$ is known to speed up the *recovery* of responses by at least two mechanisms: accelerated resynthesis of cGMP (Koch & Stryer, 1988) and reduction of the lifetime of the active form of rhodopsin (Kawamura, 1993). Obviously, such mechanisms reduce response amplitude *and* shorten the time scale. However, calcium is known to modulate several aspects of phototransduction. Lagnado and Baylor (1994) have recently reported one mechanism whereby lowered $[Ca^{2+}]_i$ reduces the gain of the activation cascade of phototransduction without affecting time scale, and others may remain to be discovered.

Acceleration in other vertebrate photoreceptors

Rods. Table 1 collects data from published work where it has been possible to extract photoreceptor t_p in at least two states of adaptation. Often only two values under background have been available; we have then *assumed* that time scale changes as a power function of background intensity, and give the exponent that would fit the data. Where possible, we have also given exponents for power functions of *sensitivity*. Many of the values have been extracted from results of single experiments. In view of this, the estimated exponents show surprisingly little variation.

Mammalian rods, however, appear to accelerate less strongly under background than rods of lower vertebrates. Although the difference may well be (partly)

TABLE 1. Response acceleration in vertebrate photoreceptors. The table gives the exponents b that best describe the acceleration of responses assuming that time scale is a power function of background intensity [equation (10), left-hand column], or a power function of flash sensitivity (right-hand column). Rod fits were restricted to backgrounds $< 10^4$ Rh* sec⁻¹. See text for details.

Species, signal	$b(t_p \propto I_B^{-b})$	$b(t_p \propto S_F^{-b})$
<i>Non-mammalian rods</i>		
1. Frog, ERG	0.19	0.35
2. Toad, photocurrent	0.23	0.41
3. Toad, photocurrent		0.38
4. Toad, photocurrent (base)	0.25	0.42
(tip)	0.28	0.37
5. <i>Triturus</i> , photocurrent	0.16	0.39
6. Skate, photocurrent		0.24
<i>Mammalian rods</i>		
7. Guinea pig, photocurrent	0.09	0.29
8. Cat, photocurrent		0.14
9. Rabbit, photocurrent	0.09	0.15
10. Human, photocurrent	0.09	0.17
11. Human, ERG <i>a</i> -wave	0.11	
<i>Cones</i>		
12. Turtle, intracellular	0.19	0.23
13. Monkey, photocurrent		0.04

Sources: 1. Present study; 2. Baylor, Lamb and Yau (1979); 3. Baylor *et al.* (1980); 4. Schnapf (1983); 5. Forti *et al.* (1989); 6. Cornwall, Ripps, Chappell and Jones (1989); 7. Matthews (1991); 8. Tamura *et al.* (1989); 9. Nakatani, Tamura and Yau (1991); 10. Kraft, Schneeweis and Schnapf (1993); 11. Hood and Birch (1993a); 12. Baylor and Hodgkin (1974); 13. Schnapf *et al.* (1990).

real, the acceleration of single mammalian photoreceptors could be underestimated. Until recently it was thought that mammalian rods lacked even sensitivity adaptation (Baylor *et al.*, 1984). It now appears that sensitivity adaptation is ubiquitous, and that failures to observe it were related to the disruptive preparative procedures associated e.g. with suction-pipette recording. Even the comparatively robust rods of amphibians adapt much less well when drawn into pipettes than in the intact retina or eyecup (Donner *et al.*, 1990). Thus it would not be surprising if kinetic adaptation could easily be partly "washed out".

Cones. Data from the literature on the time scale of linear-range cone responses are scarce. Baylor and Hodgkin (1974, their Fig. 9) present $\log t_p - \log S_F$ data for single turtle cones exposed to backgrounds. For 5 cells there are enough points (6 or more, in one case 5) over 1.5 logunits of sensitivity change under backgrounds to allow reasonably accurate fitting of power functions. The mean slope is -0.23 ± 0.07 (SD), $r^2 > 0.91$. In conjunction with the TVI function for the same cells [slope 0.82 over the relevant range, Fig. 7 in Baylor and Hodgkin (1974)], the estimated $\log t_p - \log I_B$ slope becomes -0.19 . This is a rough estimate, but it does suggest that cones do not generically behave differently from rods.

Human cones are of particular interest since a large body of relevant psychophysics (summarized in Table 2) refers to foveal cone vision. The evidence is somewhat contradictory. Current recordings from single primate cones have shown clear gain adaptation, but almost negligible acceleration under backgrounds (Schnapf,

TABLE 2. Acceleration of human foveal vision as function of mean luminance: exponents *b* that best describe the shortening of time scale as function of mean luminance (background intensity) in experiments on flicker sensitivity and "critical duration" (i.e. summation time)

Source	$b(\tau \propto I_B^{-b})$	r^2
<i>Flicker sensitivity: cutoff frequency</i>		
1. de Lange (1952)	0.16	0.97
	0.09	0.92
2. Kelly (1961)	0.17	0.98
3. Roufs (1972)	0.10	0.94
	0.17	0.93
	0.16	0.99
	0.13	0.96
Mean ± SD	0.14 ± 0.03	
<i>Critical duration</i>		
1. Graham and Kemp (1938)	0.10	0.99
2. Keller (1941) (2 subjects)	0.12	0.99
3. Herrick (1956)	0.13	0.96
	0.17	0.97
4. Roufs (1972)	0.15	0.94
	0.22	0.96
	0.18	0.99
	0.15	0.95
Mean ± SD	0.15 ± 0.04	

The values were obtained as coefficients of linear regression when fitting the data in log-log form [equation (9)]; fits restricted to luminances $\leq 3.1 \log td$. The degree of explanation is >92% in all cases, showing that the fits were fair to excellent. The time scale criterion in flicker experiments was the "cutoff frequency" defined by Roufs (1972). Unless otherwise noted, each value refers to one subject.

Nunn, Meister & Baylor, 1990). This result, however, is open to the same objections as expressed above for rods. Hood and Birch (1993b), studying the human cone ERG *a*-wave, found that the early rise of responses to a fixed flash intensity stayed virtually unchanged over a substantial range of background intensities. If it is accepted that human cones do have sensitivity adaptation, the invariance of the early rise necessarily implicates an adaptation mechanism coupled to time scale changes (see above). It then appears likely that the "photoreceptor-like" acceleration of time scale in human foveal vision (Table 2) indeed originates largely in the cones.

REFERENCES

Barlow, H. B. & Levick, W. L. (1969). Three factors limiting the reliable detection of light by retinal ganglion cells in the cat. *Journal of Physiology*, 200, 1-24.

Baylor, D. A. & Hodgkin, A. L. (1973). Detection and resolution of visual stimuli by turtle photoreceptors. *Journal of Physiology*, 214, 265-294.

Baylor, D. A. & Hodgkin, A. L. (1974). Changes in time scale and sensitivity in turtle photoreceptors. *Journal of Physiology*, 242, 729-758.

Baylor, D. A., Hodgkin, A. L. & Lamb, T. D. (1974a). The electrical response of turtle cones to flashes and steps of light. *Journal of Physiology*, 242, 685-727.

Baylor, D. A., Hodgkin, A. L. & Lamb, T. D. (1974b). Reconstruction of the electrical responses of turtle cones to flashes and steps of light. *Journal of Physiology*, 242, 759-791.

Baylor, D. A., Lamb, T. D. & Yau, K.-W. (1979). The membrane current of single rod outer segments. *Journal of Physiology*, 288, 589-611.

Baylor, D. A., Matthews, G. & Yau, K.-W. (1980). Two components of electrical dark noise in toad retinal rod outer segments. *Journal of Physiology*, 309, 591-621.

Baylor, D. A., Nunn, B. J. & Schnapf, J. L. (1984). The photocurrent, noise, and spectral sensitivity of rods of the monkey (*Macaca fascicularis*). *Journal of Physiology*, 357, 575-607.

Belgum, J. & Copenhagen, D. (1988). Synaptic transfer of rod signals to horizontal and bipolar cells in the retina of the toad. *Journal of Physiology*, 396, 225-245.

Brown, J. & Pinto, L. (1974). Ionic mechanism for the photoreceptor potential of the retina of *Bufo marinus*. *Journal of Physiology*, 236, 575-591.

Cervetto, L., Pasino, E. & Torre, V. (1977). Electrical responses of rods in the retina of *Bufo marinus*. *Journal of Physiology*, 267, 17-51.

Copenhagen, D. R., Donner, K. & Reuter, T. (1987). Ganglion cell performance at absolute threshold in frog retina: effects of dark events in rods. *Journal of Physiology*, 393, 667-680.

Cornwall, M. C., Ripps, H., Chappell, R. L. & Jones, G. J. (1989). Membrane current responses of skate photoreceptors. *Journal of General Physiology*, 94, 633-647.

Dartnall, H. J. A. (1972). Photosensitivity. In Dartnall, H. J. A. (Ed.), *Handbook of sensory physiology* (Vol. VII/1, pp. 122-145). Berlin: Springer.

Detwiler, P. B., Hodgkin, A. L. & McNaughton, P. A. (1980). Temporal and spatial characteristics of the voltage response of rods in the retina of the snapping turtle. *Journal of Physiology*, 300, 213-250.

Djupsund, K., Kouvalainen, E., Järvilehto, M. & Weckström, M. (1995). A digital feedback controller application to reveal photoreceptor adaptation by "voltage clamp by light". *Journal of Neuroscience Methods*. In press.

Donner, K. (1981). Receptive fields of frog retinal ganglion cells: response formation and light-dark adaptation. *Journal of Physiology*, 319, 131-142.

Donner, K. (1987a). Adaptation-related changes in the spatial and temporal summation of frog retinal ganglion cells. *Acta Physiologica Scandinavica*, 131, 479-487.

Donner, K. (1987b). Surround control of center adaptation in the receptive fields of frog retinal ganglion cells. *Vision Research*, 27, 1211-1221.

Donner, K. (1989). Visual latency and brightness: an interpretation based on the responses of rods and ganglion cells in the frog retina. *Visual Neuroscience*, 3, 39-51.

Donner, K., Copenhagen, D. R. & Reuter, T. (1990). Weber and noise adaptation in the retina of the toad *Bufo marinus*. *Journal of General Physiology*, 95, 733-753.

Donner, K., Hemilä, S. & Koskelainen, A. (1988). Temperature-dependence of rod photoresponses from the aspartate-treated retina of the frog (*Rana temporaria*). *Acta Physiologica Scandinavica*, 134, 535-541.

Donner, K., Hemilä, S. & Koskelainen, A. (1989). Effects of sulphhydryl binding reagents on the photoresponses of amphibian retinal rods. *Comparative Biochemistry and Physiology*, 94A, 125-132.

Donner, K., Hemilä, S. & Koskelainen, A. (1992). On the relation between ERG waves and retinal function: inverted rod photoresponses from the frog retina. *Vision Research*, 32, 1411-1416.

Fain, G. L. (1976). Sensitivity of toad rods: dependence on wavelength and background illumination. *Journal of Physiology*, 261, 71-101.

Fain, G. L. & Cornwall, M. C. (1993). Light and dark adaptation in vertebrate photoreceptors. In Shapley, R. M. & Lam, D. M.-K. (Eds), *Contrast sensitivity* (pp. 3-32). Cambridge, Mass.: The MIT Press.

Forti, S., Menini, A., Rispoli, G. & Torre, V. (1989). Kinetics of phototransduction in retinal rods of the newt *Triturus cristatus*. *Journal of Physiology*, 419, 265-295.

Fuortes, M. G. F. & Hodgkin, A. L. (1964). Changes in time scale and sensitivity in the ommatidia of *Limulus*. *Journal of Physiology*, 172, 239-263.

Graham, C. H. & Kemp, E. H. (1938). Brightness discrimination as a function of the duration of the increment in intensity. *Journal of General Physiology*, 21, 635-650.

- Gyllenberg, G., Reuter, T. & Sippel, H. (1974). Long-lived photoproducts of rhodopsin in the retina of the frog. *Vision Research*, *14*, 1349–1357.
- Hemilä, S. & Reuter, T. (1981). Longitudinal spread of adaptation in the rods of the frog's retina. *Journal of Physiology*, *310*, 501–528.
- Herrick, R. M. (1956). Foveal luminance discrimination as a function of the duration of the decrement or increment in luminance. *Journal of Comparative Physiology and Psychology*, *49*, 437–443.
- Hood, D. C. & Birch, D. G. (1993a). Light adaptation of human rod receptors: the leading edge of the human *a*-wave and models of rod receptor activity. *Vision Research*, *33*, 1605–1618.
- Hood, D. C. & Birch, D. G. (1993b). Human cone receptor activity: The leading edge of the *a*-wave and models of receptor activity. *Visual Neuroscience*, *10*, 857–871.
- Hood, D. C. & Hock, P. A. (1975). Light adaptation of the receptors: Increment threshold functions for the frog's rods and cones. *Vision Research*, *15*, 545–553.
- Kawamura, S. (1993). Rhodopsin phosphorylation as a mechanism of cyclic GMP phosphodiesterase regulation by S-modulin. *Nature (London)*, *362*, 855–857.
- Keller, M. (1941). The relation between the critical duration and intensity in brightness discrimination. *Journal of Experimental Psychology*, *28*, 407–418.
- Kelly, D. H. (1961). Visual responses to time-dependent stimuli. I. Amplitude sensitivity measurements. *Journal of the Optical Society of America*, *51*, 422–429.
- Koch, K.-W. & Stryer, L. (1988). Highly cooperative feedback control of retinal rod guanylate cyclase by calcium ions. *Nature (London)*, *334*, 64–66.
- Koskelainen, A., Hemilä, S. & Donner, K. (1994). Spectral sensitivities of short- and long-wavelength sensitive cone mechanisms in the frog retina. *Acta Physiologica Scandinavica*, *152*, 115–124.
- Kraft, T. W., Schneeweis, D. M. & Schnapf, J. L. (1993). Visual transduction in human rod photoreceptors. *Journal of Physiology*, *464*, 747–765.
- Lagnado, L. & Baylor, D. A. (1994). Calcium controls light-triggered formation of catalytically active rhodopsin. *Nature (London)*, *367*, 273–277.
- Lamb, T. D. & Pugh, E. N. Jr (1992). A quantitative account of the activation steps involved in phototransduction in amphibian photoreceptors. *Journal of Physiology*, *449*, 719–758.
- de Lange, H. (1952). Experiments on flicker and some calculations on an electrical analogue of the foveal systems. *Physica*, *18*, 935–950.
- Leibovic, K. N., Dowling, J. E. & Kim, Y. Y. (1987). Background and bleaching equivalence in steady-state adaptation of vertebrate rods. *Journal of Neuroscience*, *7*, 1056–1063.
- Matthews, H. (1991). Incorporation of chelator into guinea-pig rods shows that calcium mediates mammalian photoreceptor light adaptation. *Journal of Physiology*, *436*, 93–105.
- Nakatani, K., Tamura, T. & Yau, K.-W. (1991). Light adaptation in retinal rods of the rabbit and two other nonprimate mammals. *Journal of General Physiology*, *97*, 413–435.
- Pugh, E. N. Jr & Lamb, T. D. (1990). Cyclic GMP and calcium: The internal messengers of excitation and adaptation in vertebrate photoreceptors. *Vision Research*, *30*, 1923–1948.
- Reuter, T., Donner, K. & Copenhagen, D. R. (1986). Does the random distribution of discrete photoreceptor events limit the sensitivity of the retina? *Neuroscience Research, Suppl.* *4*, S163–S180.
- Roufs, J. A. J. (1972). Dynamic properties of vision—I. Experimental relation between flicker and flash thresholds. *Vision Research*, *12*, 261–278.
- Sakmann, B. & Fillion, M. (1972). Light adaptation of the late receptor potential in the cat retina. In Arden, G. B. (Ed.), *The visual system. Neurophysiology, biophysics and their clinical applications* (pp. 87–93). New York: Plenum.
- Schnapf, J. L. (1983). Dependence of the single-photon response on longitudinal position of absorption in toad rod outer segments. *Journal of Physiology*, *343*, 147–159.
- Schnapf, J. L. & Copenhagen, D. R. (1982). Differences in the kinetics of rod and cone synaptic transmission. *Nature (London)*, *296*, 862–864.
- Schnapf, J. L., Nunn, B. J., Meister, M. & Baylor, D. A. (1990). Visual transduction in cones of the monkey *Macaca fascicularis*. *Journal of Physiology*, *427*, 681–713.
- Schwartz, E. A. (1976). Electrical properties of the rod syncytium in the retina of the turtle. *Journal of Physiology*, *257*, 379–406.
- Shapley, R. & Enroth-Cugell, C. (1984). Visual adaptation and retinal gain controls. In Osborne, N. & Chader, G. (Eds), *Progress in retinal research* (Vol. 3, pp. 263–346). Oxford: Pergamon Press.
- Sharpe, L. T., Stockman, A., Fach, C. C. & Markstahler, U. (1993). Temporal and spatial summation in the human rod visual system. *Journal of Physiology*, *463*, 325–348.
- Sharpe, L. T., Stockman, A. & MacLeod, D. (1989). Rod flicker perception: Scotopic duality, phase lags and destructive interference. *Vision Research*, *29*, 1539–1559.
- Steinberg, R. (1971). Incremental responses to light recorded from pigment epithelial cells and horizontal cells of the cat retina. *Journal of Physiology*, *217*, 93–110.
- Steinberg, R., Reid, M. & Lacy, P. L. (1973). The distribution of rods and cones in the retina of the cat (*Felis domesticus*). *Journal of Comparative Neurology*, *148*, 229–248.
- Tamura, T., Nakatani, K. & Yau, K.-W. (1989). Light adaptation in cat retinal rods. *Science*, *245*, 755–758.
- Tomita, T. & Yanagida, T. (1981). Origins of the ERG waves. *Vision Research*, *21*, 1703–1707.

Acknowledgements—We wish to thank Mr Antti Miettinen for skilful technical assistance and Professor Tom Reuter for critically reading the manuscript. This work was supported by the Academy of Finland (Grant 01/1011872).